

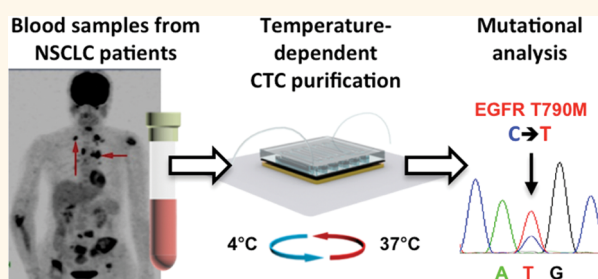
# Programming Thermoresponsiveness of NanoVelcro Substrates Enables Effective Purification of Circulating Tumor Cells in Lung Cancer Patients

Zunfu Ke,<sup>\*,†,‡,¶</sup> Millicent Lin,<sup>†,‡,¶</sup> Jie-Fu Chen,<sup>‡</sup> Jin-sil Choi,<sup>‡</sup> Yang Zhang,<sup>‡</sup> Anna Fong,<sup>‡</sup> An-Jou Liang,<sup>‡</sup> Shang-Fu Chen,<sup>‡</sup> Qingyu Li,<sup>‡</sup> Wenfeng Fang,<sup>‡</sup> Pingshan Zhang,<sup>‡</sup> Mitch A. Garcia,<sup>‡</sup> Tom Lee,<sup>‡</sup> Min Song,<sup>‡</sup> Hsing-An Lin,<sup>§</sup> Haichao Zhao,<sup>§</sup> Shyh-Chyang Luo,<sup>§,||</sup> Shuang Hou,<sup>\*,‡</sup> Hsiao-hua Yu,<sup>\*,§,⊥</sup> and Hsian-Rong Tseng<sup>\*,‡</sup>

<sup>†</sup>Department of Pathology, The First Affiliated Hospital of Sun Yat-Sen University, Guangzhou, Guangdong 510080, P.R. China, <sup>‡</sup>Department of Molecular and Medical Pharmacology, Crump Institute for Molecular Imaging (CIMI), California NanoSystems Institute (CNSI), University of California, Los Angeles, California 90095, United States, <sup>§</sup>Responsive Organic Materials Laboratory, RIKEN, 2-1 Hirosawa, Wako, Saitama 351-0198, Japan, <sup>||</sup>Department of Materials Science and Engineering, National Cheng Kung University, Tainan 70101, Taiwan, and <sup>⊥</sup>Institute of Chemistry, Academia Sinica, 128 Academia Road Sec. 2, Nankang, Taipei 115, Taiwan. \*These authors (Z.K. and M.L.) contributed equally to this work.

**ABSTRACT** Unlike tumor biopsies that can be constrained by problems such as sampling bias, circulating tumor cells (CTCs) are regarded as the “liquid biopsy” of the tumor, providing convenient access to all disease sites, including primary tumor and fatal metastases. Although enumerating CTCs is of prognostic significance in solid tumors, it is conceivable that performing molecular and functional analyses on CTCs will reveal much significant insight into tumor biology to guide proper therapeutic intervention. We developed the Thermoresponsive NanoVelcro CTC

purification system that can be digitally programmed to achieve an optimal performance for purifying CTCs from non-small cell lung cancer (NSCLC) patients. The performance of this unique CTC purification system was optimized by systematically modulating surface chemistry, flow rates, and heating/cooling cycles. By applying a physiologically endurable stimulation (*i.e.*, temperature between 4 and 37 °C), the mild operational parameters allow minimum disruption to CTCs' viability and molecular integrity. Subsequently, we were able to successfully demonstrate culture expansion and mutational analysis of the CTCs purified by this CTC purification system. Most excitingly, we adopted the combined use of the Thermoresponsive NanoVelcro system with downstream mutational analysis to monitor the disease evolution of an index NSCLC patient, highlighting its translational value in managing NSCLC.



**KEYWORDS:** cancer diagnosis · circulating tumor cells · nanostructured materials · thermoresponsive polymer · non-small cell lung cancer

Circulating tumor cells<sup>1,2</sup> (CTCs) are cancer cells that break away from either primary tumor or metastatic sites and circulate in the peripheral blood as the cellular origin of metastasis. Although detecting and enumerating<sup>3–5</sup> CTCs is of prognostic significance in different types of solid tumors, it is conceivable that performing molecular<sup>6–9</sup> and functional<sup>10,11</sup> analyses on CTCs will reveal insights into tumor biology during the critical window, where therapeutic intervention could make a significant difference. To pave the way for obtaining CTC-derived molecular signatures<sup>6–9</sup> and functional readouts,<sup>10,11</sup> it is

important to develop novel methodologies that can recover CTCs with minimum contamination of white blood cells (WBCs) and negligible disruption to their viabilities.

We pioneered a unique concept of “NanoVelcro” cell-affinity assays,<sup>12–16</sup> in which capture agent (*e.g.*, anti-EpCAM)-coated nanostructured substrates were utilized to achieve enhanced affinities with CTCs, resulting in desired cell-capture efficiency. In addition to silicon nanowire substrates (SiNWS),<sup>12</sup> the general applicability of NanoVelcro assays is also supported by our<sup>13–15</sup> and others<sup>17–23</sup> research endeavors, where a diversity of nanostructured materials was

\* Address correspondence to kezunfu@mail.sysu.edu.cn, shuanghou@mednet.ucla.edu, bruceyu@gate.sinica.edu.tw, HRTseng@mednet.ucla.edu.

Received for review October 2, 2014 and accepted December 13, 2014.

Published online December 13, 2014  
10.1021/nn5056282

© 2014 American Chemical Society

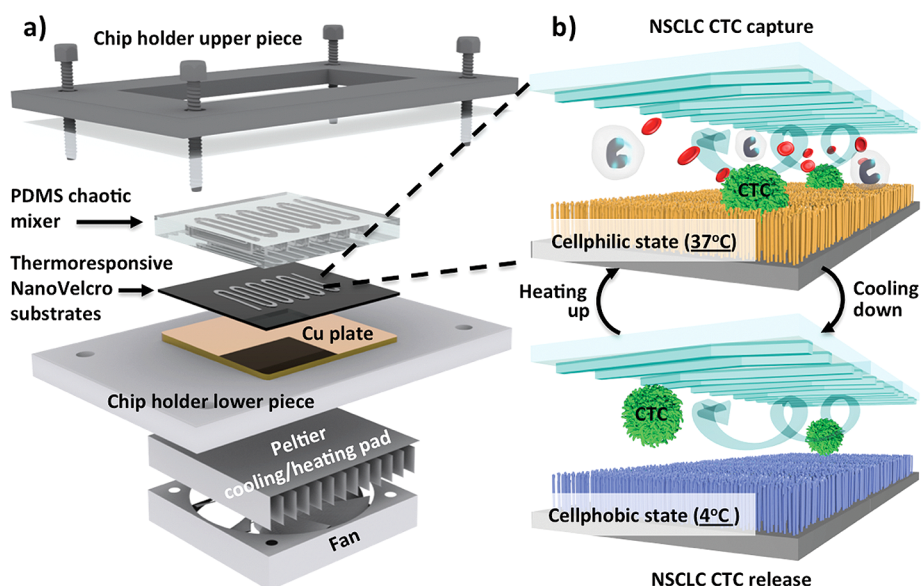


**Figure 1.** Thermoresponsive NanoVelcro system for purification of NSCLC CTCs. (a) Chip holder is employed to assemble a lithographically patterned Thermoresponsive NanoVelcro substrate with an overlaid PDMS chaotic mixer. A Peltier cooling/heating pad (integrated with a thermocouple sensor) is located underneath the lower piece of the chip holder, enabling instant and precise temperature control of the system. (b) At 37 °C, the Thermoresponsive NanoVelcro substrate is programmed to its “cellphilic” state. The chaotic mixer is capable of enhancing the contact frequency between the flowing-through NSCLC CTCs and the substrate, leading to an improved CTC-capture performance. The substrate can defectively release CTCs at its “cellphobic” state (4 °C). Multiple heating/cooling cycles can further increase the efficiency of CTC release.

combined with capture agents to achieve highly efficient detection of CTCs as well as other types of rare cells. Over the past 5 years, several categories<sup>16</sup> of NanoVelcro CTC chips have been demonstrated by our research team to meet needs in oncology clinics. First, in the presence of anti-EpCAM, NanoVelcro chips<sup>24,25</sup> with embedded SiNWS and overlaid microfluidic chaotic mixers<sup>26</sup> were developed for CTC detection and enumeration. To implement molecular analyses on CTCs, we then established the combined use of transparent polymer NanoVelcro chips<sup>27,28</sup> and laser capture microdissection (LCM) technique, enabling a great precision for single-CTC isolation as well as subsequent mutational analysis<sup>27</sup> and genomic sequencing.<sup>28</sup> For supporting routine clinical applications, challenges remain to further simplify the labor-consuming process and improve the viability of the isolated CTCs encountered by the NanoVelcro-LCM approach.<sup>27,28</sup> Thermoresponsive NanoVelcro substrates<sup>29</sup> were developed to address these issues. By grafting thermoresponsive polymer brushes<sup>30</sup> (*i.e.*, poly(*N*-isopropylacrylamide, PIPAAm) onto SiNWS, Thermoresponsive NanoVelcro substrates can capture and release CTCs at 37 and 4 °C, respectively. The temperature-dependent conformational changes of polymer brushes can alter the accessibility of the capture agent (*i.e.*, anti-EpCAM) on the NanoVelcro, allowing reversible switches between the “cellphilic” and “cellphobic” states of the NanoVelcro substrates.

On the basis of the stationary Thermoresponsive NanoVelcro substrates,<sup>29</sup> we foresaw that further improvement of cell purification performance could be

achieved by increasing the contact frequency between CTCs and NanoVelcro substrates, as well as fast temperature responsiveness (Figure 1). With the incorporation of an overlaid polydimethylsiloxane (PDMS) chaotic mixer<sup>26,31</sup> onto a lithographically patterned Thermoresponsive NanoVelcro substrate, we developed the Thermoresponsive NanoVelcro chip (Figure 1b) with improved CTC-capture performance. Further, in order to instantly and precisely control devices' responsiveness at different temperatures, we machined a chip holder to integrate a thermo-electric Peltier cooling/heating system with a built-in thermocouple sensor (see its heating/cooling performance in Figure S1 in Supporting Information). As a result, operational parameters (*i.e.*, flow rates and cooling/heating of such Thermoresponsive NanoVelcro system) can be digitally programmed to achieve an optimal performance for purifying CTCs, while preserving the CTCs' viability and molecular integrity. We showed that our Thermoresponsive NanoVelcro CTC purification system could be utilized to purify non-small cell lung cancer (NSCLC) CTCs from both artificial and clinical blood samples, enabling subsequent cell culture and mutational analyses. In contrast to the other NanoVelcro CTC assays<sup>16</sup> demonstrated by our research team, the overall improvement of this Thermoresponsive NanoVelcro CTC purification system is explicitly illustrated in Table S1 (see Supporting Information).

Lung cancer is the major cause of cancer-related death worldwide,<sup>32</sup> and NSCLC accounts for approximately 70–80% of incidents.<sup>33</sup> A substantial portion of NSCLC patients present with oncogenic driver mutations in

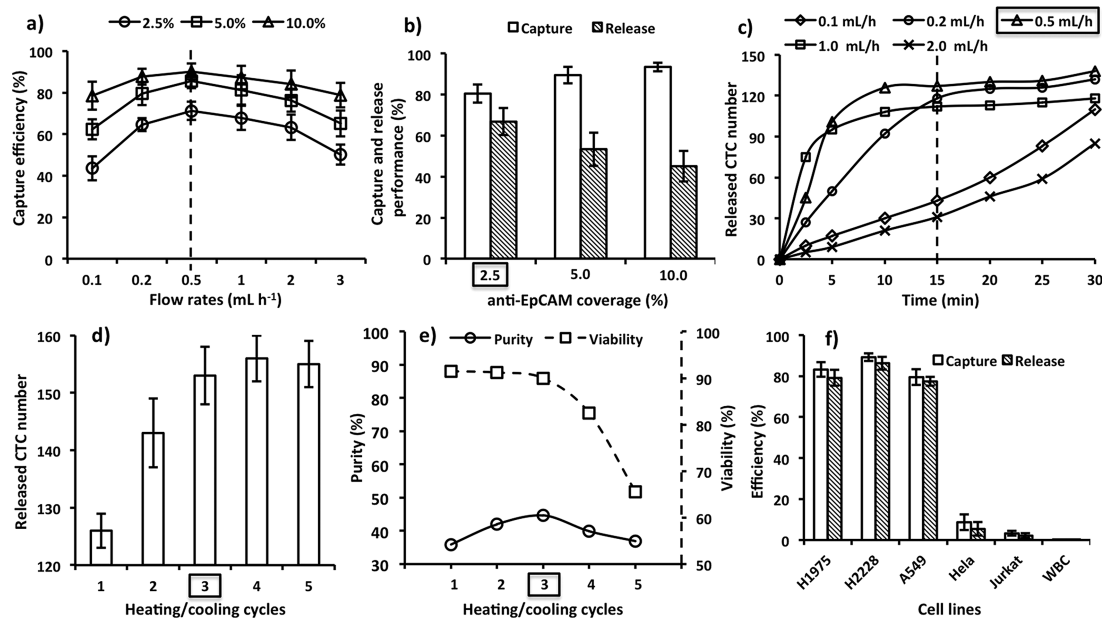


**Figure 2.** Optimization of operational parameters for purifying NSCLC CTCs. (a) At 37 °C, variable cell-capture efficiencies were observed for three anti-EpCAM surface coverages (2.5, 5, and 10%) at different flow rates. The 0.5 mL h<sup>-1</sup> flow rate gave the best cell-capture performance. (b) Cell-capture and release performances were observed for different anti-EpCAM coverages at 37 and 4 °C, respectively. (c) At 2.5% of anti-EpCAM coverage, differential cell-release performances were observed for different flow rates at 4 °C. The 0.5 mL h<sup>-1</sup> flow rate gave the best cell-release performance. (d) At an optimal cell-release condition, improved performances were observed with increased heating/cooling cycles. It required at least three heating/cooling cycles to effectively release the substrate-immobilized cells. (e) Heating/cooling cycles affected the viability and purity of recovered cells. (f) Performance observed for capturing and releasing EpCAM-positive NSCLC cell lines (*i.e.*, H1975, H2228, and A549) and EpCAM-negative cells (*i.e.*, HeLa, Jurkat, and WBCs).

epidermal growth factor receptor (EGFR) genes, leading to the response to the targeted therapy known as EGFR tyrosine kinase inhibitors (EGFR TKIs, *e.g.*, gefitinib),<sup>34</sup> which offers significant survival benefit to these patients. To guide the implementation of EGFR TKI treatment, invasive biopsy or surgery is employed to collect NSCLC tissues for characterizing the presence of these EGFR mutations. However, these invasive sampling procedures impose significant risk to the patients. As an alternative, CTCs can be repetitively sampled and analyzed in a minimally invasive manner, thus allowing real-time monitoring of the evolution of tumor driver mutations. We demonstrated that a small number of CTCs purified by the Thermoresponsive NanoVelcro system could be first subjected to amplifications of their genomic DNA, followed by Sanger sequencing to detect EGFR point mutations.

## RESULTS AND DISCUSSION

Thermoresponsive NanoVelcro substrates were prepared through two continuous steps, including (i) photolithography and wet etching to introduce<sup>24,25</sup> vertically aligned SiNWS onto a silicon wafer and (ii) covalently grafting<sup>29</sup> PIPAAm polymer brushes that confer “thermoresponsiveness” to the devices. Biotin–streptavidin-mediated conjugation<sup>29</sup> was employed to introduce NSCLC CTC-specific capture agent (*i.e.*, anti-EpCAM) onto NanoVelcro substrates (see fabrication details in Supporting Information Figures S2–S5). SEM

surface characterizations (Figure S6) and temperature-dependent contact angle measurements of water droplets (Figure S7) were utilized to examine the thermo-responsive surface properties of these PIPAAm-grafted SiNWS. By controlling the mixing ratios of PIPAAm precursors,<sup>24,25</sup> three different biotin densities (*i.e.*, 2.5, 5.0, and 10.0%) were obtained, giving control of anti-EpCAM densities on NanoVelcro substrates. In order to optimize the operation parameters for CTC purification by the Thermoresponsive NanoVelcro system, the first-type artificial CTC sample containing EpCAM-positive H1975 NSCLC cells (200 cells mL<sup>-1</sup>) and freshly purified human WBCs (5 × 10<sup>6</sup> WBCs mL<sup>-1</sup>) in a RPMI medium was prepared. For the convenience of cell counting, H1975 cells were prestained with DiO green fluorescent dye.

We first examined how the anti-EpCAM coverage and flow rates affected cell-capture performance of the Thermoresponsive NanoVelcro system under the cellphilic temperature (*i.e.*, 37 °C). After the substrate-immobilized cells were counted under a fluorescence microscope (Nikon, 90i), the results summarized in Figure 2a suggest that, at the flow rate of 0.5 mL h<sup>-1</sup>, optimal cell-capture performance was achieved for all the three different anti-EpCAM coverages. We then studied how anti-EpCAM coverages (Figure 2b) and release flow rates/duration time (Figure 2c) affected the cell-release behaviors of the system. For these studies, H1975 cells were first immobilized on the

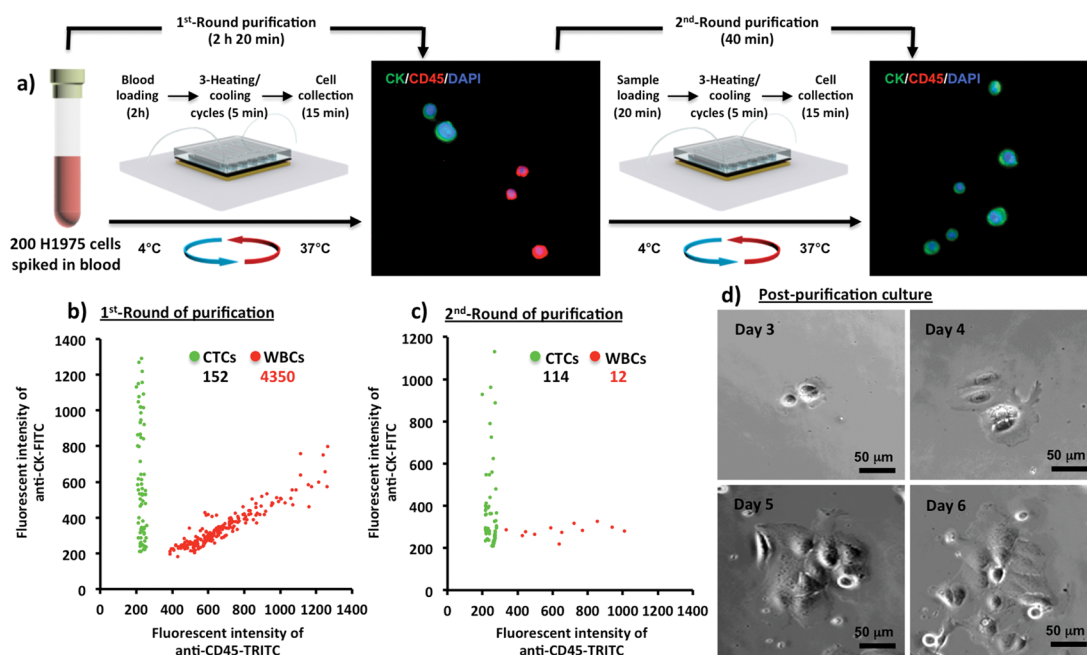


**Figure 3.** Two rounds of CTC purification, followed by culture expansion. (a) Workflow summarizes two rounds of CTC purification using the Thermo-responsive NanoVelcro system. Fluorescent micrographs showed that the purities of recovered CTCs (CK+/CD45−/DAPI+) gradually improved over the first and second rounds of purification processes. The scatter plots conclude H1975/WBC cell distribution observed for one of the cell suspensions after the (b) first and (c) second rounds of CTC purification process. (d) Bright-field micrographs of double-purified H1975 cells cultured over a period of 2 weeks.

substrates by flowing ( $0.5 \text{ mL h}^{-1}$ ) the artificial CTC sample into the chips. We note that the majority of cells were captured in the first four channels of the anti-EpCAM-modified chips (Figure S8a). The results shown in Figure 2b suggested that the chips with 2.5% anti-EpCAM coverage exhibited the best cell-release performance. For the chips with higher anti-EpCAM coverages (*i.e.*, 5 and 10%), their cell-release performances were less impressive due to the fact that the cells released from their initially captured locations were subsequently “recaptured” on a later portion of the microchannel. We attributed this observation to the incomplete switches of polymer brushes from their cellphilic to cellphobic states. Although applying lower anti-EpCAM coverages (2.5%, Figure 2b) and proper flow rates ( $0.5 \text{ mL h}^{-1}$ , Figure 2c) enhanced cell-release performance, further improvement could be achieved by applying “multiple heating/cooling cycles” (see Figure 2d,e). Prior to infusing RMPI media ( $0.5 \text{ mL h}^{-1}$ ,  $4^\circ\text{C}$ ) to collect the released cells, the device temperatures were quickly switched between 37 and  $4^\circ\text{C}$  for multiple cycles, resulting in more complete switching to their cellphobic states. Figure 2d suggests that it requires at least three heating/cooling cycles (between 37 and  $4^\circ\text{C}$ ) to effectively release CTCs from NanoVelcro substrates at  $4^\circ\text{C}$ . Taking the impact on cell purity and viability into account (Figure 2e), we determined that three-round heating/cooling cycles ( $<3 \text{ min}$ ) would effectively release immobilized CTCs. Overall, the improved operation protocol enables temperature-dependent CTC purification in a period  $<1.5 \text{ h}$ , with  $>70\%$  recovery yield,

$>35\%$  purity, and  $>90\%$  cell viability (Figure 2e). This condition is generally applicable (Figure 2f) to three EpCAM-expressing NSCLC cells (*i.e.*, H1975, H2228, and A549) in contrast to non-EpCAM-expressing cells (*i.e.*, HeLa, Jurkat, and WBCs).

Under the optimized condition determined above, the Thermo-responsive NanoVelcro system was tested using the second-type artificial blood samples prepared by spiking 200 H1975 NSCLC cells into 1.0 mL of healthy donors' blood. The blood samples were introduced (Figure 3a) into the chips at  $37^\circ\text{C}$  at a flow rate of  $0.5 \text{ mL h}^{-1}$ . After three rounds of heating/cooling cycles, the specifically captured H1975 cells were released at  $4^\circ\text{C}$  under a flow rate of  $0.5 \text{ mL h}^{-1}$  for 15 min. After parallel staining of FITC-labeled anti-CK, TRITC-labeled anti-CD45, and DAPI, the purified cells were counted in a 96-well plate by a fluorescence microscope. A scatter plot (Figure 3b) was generated to summarize one of the experimental outcomes ( $n = 3$ ), where  $152 \pm 4$  H1975 NSCLC cells (CK+/CD45−/DAPI+) and 2400–5000 WBCs (CK−/CD45+/DAPI+) were identified in the recovered cell suspension. In contrast to the CTC purities shown in Figure 2e, the reduced CTC purities in these studies may be attributed to more complex background (presence of both RBCs and WBCs) in the whole blood. By repeating the CTC purification for a second round (Figure 3a), the purity of CTCs was further improved to 88–98% (Figure 3c), and the improved purity allowed for implementation of subsequent cell expansion and mutational analysis. The viability of these double-purified

**TABLE 1. Detailed Clinical Characteristics of the Seven NSCLC Patients Who Participated in Our Studies<sup>a</sup>**

| patient | sex | smoking    |               | tumor<br>origin | adenocarcinoma<br>subtype | tumor<br>grade | clinical<br>stage | node<br>status | total CTCs <sup>b</sup><br>(per 1 mL<br>blood) | L858R<br>mutation<br>(tissue) | L858R<br>mutation<br>(CTC) | T790M<br>mutation<br>(tissue) | T790M<br>mutation<br>(CTC) |
|---------|-----|------------|---------------|-----------------|---------------------------|----------------|-------------------|----------------|--|-------------------------------|----------------------------|-------------------------------|----------------------------|
|         |     | age<br>(y) | status<br>(y) |                 |                           |                |                   |                |  |                               |                            |                               |                            |
| P1      | M   | 51         | 12            | pleura (MS)     | acinar and papillary      | 3              | III               | positive       | 6  | +                             | +                          | –                             | –                          |
| P2      | M   | 64         | 0             | lung (PT)       | solid                     | 3              | IV                | negative       | 7  | +                             | +                          | –                             | –                          |
| P3      | F   | 68         | 0             | lung (PT)       | mucinous                  | 1              | III               | positive       | 5  | +                             | +                          | –                             | –                          |
| P4      | F   | 69         | 3             | lung (PT)       | mucinous                  | 2              | III               | positive       | 3  | +                             | +                          | –                             | –                          |
| P5      | F   | 41         | 15            | lung (PT)       | solid                     | 2              | III               | positive       | 2  | +                             | +                          | –                             | –                          |
| P6 (BT) | M   | 75         | 47            | pleura (MS)     | mucinous                  | 3              | IV                | positive       | 9  | +                             | +                          | –                             | –                          |
| P6 (AR) | M   | 75         | 47            | pleura (MS)     | mucinous                  | 3              | IV                | positive       | 17   | –                             | –                          | +                             | +                          |
| P7      | F   | 51         | 0             | lung (PT)       | mucinous                  | 3              | III               | negative       | 4  | –                             | –                          | +                             | +                          |

<sup>a</sup> Abbreviations: CTC, circulating tumor cell; F, female; M, male; MS, metastatic site; PT, primary tumor; y, years; L858R, a single amino acid substitution from leucine to arginine at codon 858; T790M, a single amino acid substitution from threonine to methionine at codon 790; BT, before treatment; AR, at relapse. <sup>b</sup> Total numbers of CTCs per 1 mL of blood were obtained by performing 3-color immunocytochemistry on the purified CTCs (in aliquot samples), followed by counting the CTC events (CK+/CD45–/DAPI+) under a fluorescence microscope.

H1975 cells was around 85% upon examination and was further demonstrated by culture expansion in RPMI medium was for over 2 weeks (Figure 3d).

To examine the feasibility of mutational analysis on the purified CTCs, we first performed mutational analysis on the EGFR gene (Figure S9) using the second-type artificial blood sample. We note that the H1975 cells constitute a good model system for this feasibility study, as they carry both L858R and T790M EGFR point mutations. The L858R point mutation is the most common oncogenic driver mutation in NSCLCs. It represents the tumor's susceptibility to EGFR TKIs and is used to guide the implementation of EGFR TKI treatment.<sup>34</sup> On the other hand, T790M point mutation arises after the patient's initial responses to EGFR TKI treatment, indicating the development of resistance to EGFR TKIs<sup>35</sup> and the necessity of administering new-generation EGFR TKIs (*e.g.*, AZD9291<sup>36</sup> and CO-1686<sup>37</sup>). Supported by the feasibility study, we collected blood samples from seven NSCLC patients (stages III–IV; see Table 1), whose tumors harbored either L858R or T790M point mutations in the EGFR gene (confirmed by tissue-based PCR and Sanger sequencing; see Table S3). For each NSCLC patient, two 1.0 mL blood samples were subjected to the two-round purification protocol (Figure 4a) in the Thermoresponsive NanoVelcro system to obtain purified CTC samples. One of the purified CTC samples was subjected to a CTC enumeration study (Table 1 and Supporting Information) and the other one to DNA amplification by whole genome amplification (WGA) kit (REPLI-g, Qiagen). Subsequently, primers (sequences provided in Table S1) spanning *EGFR* exon 20 (covering codon 790) and 21 (covering codon 858) were used to amplify the resulting WGA DNA by PCR. The amplified DNA was then sent for Sanger sequencing. Either L858R or T790M mutation was detected in the CTCs that were purified from the seven NSCLC patients' blood samples. The mutations identified in the CTCs were

consistent with those found in the matching tumor tissues (see Table 1 and Table S2).

To further explore the clinical utility and value of serial CTC-based mutational analyses in NSCLC, we adopted our approach (Figure 4a) to monitor the disease evolution of an index NSCLC patient (patient 6 in Table 1), whose EGFR mutations underwent a significant change before and after the patient's gefitinib treatment. A blood sample was collected from the patient for our CTC-based mutational analysis prior to his gefitinib treatment. At that time, the patient presented with a heavy tumor burden (Figure 4b-I). The sequencing results of the CTCs purified by the Thermoresponsive NanoVelcro system (Figure 4c) showed L858R EGFR mutation with a strong signal-to-noise ratio, which is consistent with the sequencing results of the tumor tissue (Table S2). The patient responded to gefitinib for about 4 months, and shrinkage of the tumor was noted radiographically (Figure 4b-II). Later, the disease relapsed (Figure 4b-III). At the time of disease relapse, CTC-based mutational analysis showed the evolution of the EGFR mutations (Figure 4d) from L858R to T790M, which correlated well with the newly developed resistance to the EGFR TKI treatment. The result suggests the potential role of our CTC-based mutational analysis approach for guiding the implementation of targeted treatments at the crucial timing of NSCLC progression.

## CONCLUSIONS

Based on our extensive research experience on developing NanoVelcro-embedded CTC assays,<sup>16</sup> we introduced the Thermoresponsive NanoVelcro CTC purification system capable of purifying CTCs from NSCLC patients. The performance of this unique CTC purification system was optimized by systematically modulating surface chemistry, flow rates, and heating/cooling cycles. By applying a physiologically endurable

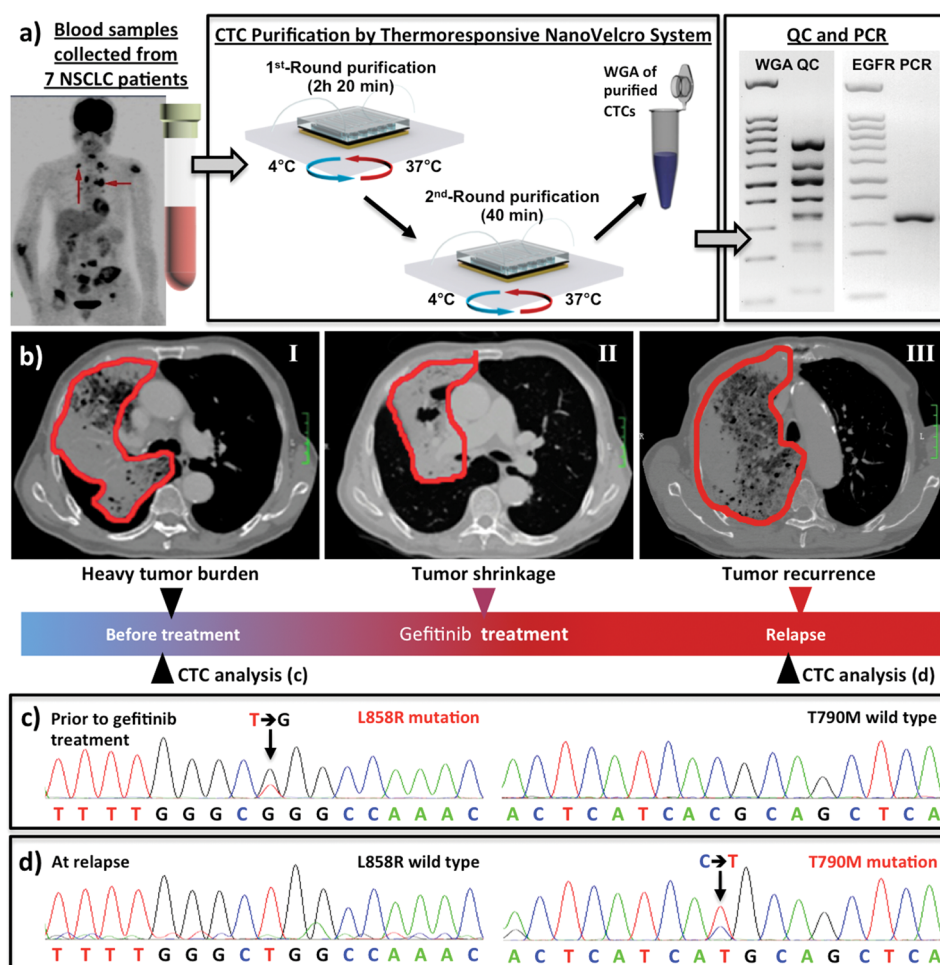


**Figure 4.** Monitoring evolution of EGFR mutations in a NSCLC patient. (a) Workflow summarizes CTC-based EGFR mutational analysis using patients' blood samples, starting from thermoresponsive CTC purification of blood samples, via PCR amplifications and QC of CTC-derived DNA, to Sanger sequencing targeting L858R and T790M point mutations in EGFR gene. (b) Three computed tomography (CT) scans of patient 6 taken at the timings of (I) heavy tumor burden before the patient's gefitinib treatment, (II) tumor shrinkage 3 months post-treatment, and (III) tumor relapse as a result of developing resistance to gefitinib. (c,d) Sanger sequencing data observed for the same patient before his gefitinib treatment and at the time of tumor relapse. L858R or T790M mutation was detected in the purified CTCs before treatment and at the time of tumor relapse, respectively.

stimulation (*i.e.*, temperature between 4 and 37 °C), the mild operational parameters allow minimum disruption to CTCs' viability and molecular integrity. Consequently, we were able to successfully demonstrate culture expansion and mutational analysis of the NSCLC CTCs purified by our thermoresponsive CTC

purification system. Most excitingly, we adopted the combined use of the Thermoresponsive NanoVelcro system with downstream mutational analysis to monitor the disease evolution of an index NSCLC patient, highlighting its translational value in managing NSCLC with underlying EGFR mutations.

## METHODS

**Materials.** Fabrication of Silicon Nanowire Substrates (SiNWS). Silicon wafers (p-type, (100)-orientation, resistivity of ca. 10–20 Ω·cm) were acquired from Silicon Quest Int'l. Sulfuric acid (98%), hydrogen peroxide (30%), silver nitrate (>99.8%), hydrofluoric acid (48%), ethanol (>99.5%), and 3-mercaptopropyl trimethoxysilane (95%) were purchased from Sigma-Aldrich Co.

**Polymer Brush Synthesis and Conjugation.** Anhydrous toluene, dichloromethane, *N,N*-dimethylformamide, triethylamine, 3-aminopropyltriethoxysilane (APTES, 98%), copper(I) bromide (98%), 2-bromo-2-methylpropionyl bromide (98%),

*N*-(3-(dimethylamino)propyl)-*N'*-ethylcarbodiimide hydrochloride (EDC, ≥98%), biotin (97%), and 2-aminoethyl methacrylate hydrochloride were obtained from Sigma-Aldrich. *N*-Isopropylacrylamide (NIPAM, >98.0%) was purchased from TCI. All chemicals were used without additional purification.

**Cell Studies.** The acute T cell leukemia cell line (Jurkat), cervical cancer cell line (HeLa), and non-small-cell lung cancer cell lines (H1975, A549, and H2228) were from American Type Culture Collection. With UCLA IRB's approval (#00000173), we isolated white blood cells from the healthy donors' blood samples. DMEM F12, GlutaMAX-I, Hoechst 33342, RPMI-1640 culture medium, Vybrant DiD, and DiO cell-labeling solutions

were obtained from Invitrogen (Cat# V-22889). Biotinylated human anti-EpCAM/TROP1 antibody (goat IgG) and streptavidin ( $1 \text{ mg mL}^{-1}$ ) were from R&D systems. Fetal bovine serum was obtained from Lonza BioWhittaker. Sodium citrate (10% w/w, Sigma-Aldrich) was used to avoid coagulation during blood collection. Acridine orange/ethidium bromide (AO/EB, Cat# A3568/Cat# E1374) was from Invitrogen and used for dual-fluorescent cell viability assay. One microliter of acridine orange stock ( $5 \text{ mg mL}^{-1}$  in ethanol) and  $1 \mu\text{L}$  of ethidium bromide stock ( $3 \text{ mg mL}^{-1}$  in ethanol) were mixed together in  $1 \text{ mL}$  of phosphate-buffered saline (PBS) as AO/EB working solution.

**Fabrication of PDMS Chaotic Mixer.** PDMS chaotic mixers were fabricated based on a soft lithographic approach.<sup>38,39</sup> The patterned silicon master mold (or silicon replicate) was fabricated by a standard two-step photolithographic procedure. A negative photoresist (SU8-2100, MicroChem Corp., Newton, MA, USA) was spin-coated with a  $100 \mu\text{m}$  thickness onto a 3 in. silicon wafer. After exposure to UV and further development, a serpentine fluidic channel with a rectangular cross shape (length  $22 \text{ cm}$  and width  $1.0 \text{ mm}$ ) was obtained. Another negative photoresist ( $35 \mu\text{m}$ , SU8-2025, MicroChem Corp.) was spin-coated on the same wafer. Prior to UV irradiation, the mask was aligned (Karl Suss America Inc., Waterbury, VT, USA) to get an accurate alignment between the prior pattern and the pattern to be imprinted. The fabricated pattern contained ceiling "ridges" that promote chaotic mixing effect in the fluid channel. The mold was then exposed to trimethylchlorosilane vapor for 2–3 min and then transferred to a Petri dish. To prepare a  $6 \text{ mm}$  thick chip, a well-mixed PDMS prepolymer (GE Silicones, Waterford, NY, USA; RTV 615 A and B in 10 to 1 ratio) was poured into the mold and kept in an oven at  $80 \text{ }^\circ\text{C}$  for 48 h. The PDMS chaotic mixers were then peeled off from the mold, and two through-holes were punched at the fabric channel's ends for connection with the fluidic handler.

**Preparation of Thermoresponsive NanoVelcro Substrates.** *Photolithography and Wet Etching To Introduce<sup>24,25</sup> SiNWS onto a Silicon Wafer.* Lithographically patterned SiNWS were prepared by a standard photolithography and a chemical wet etching process.<sup>40</sup> Photoresist (AZ 5214) was spin-coated onto a silicon wafer with  $100 \mu\text{m}$  thickness. After exposure of UV light and development, the silicon wafer was kept in etching solution containing deionized water, HF (4.6 M), and silver nitrate (0.2 M). Then, the substrate was treated with boiling aqua regia (3:1 (v/v) HCl/HNO<sub>3</sub>) for 15 min. The patterned photoresist on the silicon substrate was removed by rinsing with acetone and ethanol. After being washed with deionized water and then dried with nitrogen, the patterned SiNWS were obtained.

*Covalently Grafting<sup>29</sup> PIPAAm Polymer Brushes onto SiNWS.* The surfaces of the lithographically patterned SiNWS were modified with APTES (1% (v/v) in toluene) to have amine groups. The APTES-grafted SiNWS were reacted with 2-bromo-2-methylpropionyl bromide (9.1 mL, 72 mmol, atom transfer radical polymerization (ATRP) initiator) in the solution of dichloromethane (200 mL) and triethylamine (10 mL, 72 mmol). Then, NIPAM and 2-aminoethyl methacrylate hydrochloride were polymerized on the surface of the ATRP initiator conjugated SiNWS in the presence of Cu(I)Br. PIPAAm containing three different amine group densities (*i.e.*, 2.5, 5.0, and 10.0%) were obtained by controlling the mixing ratios of copolymer precursors. Finally, biotin (0.48 g, 1.9 mmol) was conjugated on PIPAAm-grafted SiNWS via EDC reaction.

**Characterization Methods and Settings.** *Scattering Electron Microscope (SEM).* The biotin-grafted SiNWS were confirmed with SEM (JSM-6330F, JEOL, 10 keV). The samples were coated with gold ( $<3 \text{ nm}$ ) prior to examination with a FE-SEM.

*Contact Angle Measurement System.* The contact angle of the water droplet on biotin-grafted SiNWS was measured at 37 and  $4 \text{ }^\circ\text{C}$  using contact angle measurement system (SImage mini, Excimer, Inc.) containing a heating/freezing stage (Linkam Scientific Instrument). The contact angle of  $1.5 \mu\text{L}$  of deionized water was measured three times at each temperature.

*Fluorescent Microscopy, Imaging Processing, and Data Analysis.* The Ad-SiNW chip was mounted onto a Nikon TE2000S inverted fluorescent microscope with a CCD camera (QImaging, Retiga 4000R), X-Cite 120 mercury lamp, automatic stage, and

filters for five fluorescent channels ( $W_1$ , 325–375 nm;  $W_2$ , 465–495 nm;  $W_3$ , 570–590 nm;  $W_4$ , 590–650 nm; and  $W_5$ , 650–900 nm).

**Preparation of an Artificial CTC Sample.** The first-type artificial CTC sample containing EpCAM-positive H1975 NSCLC cells ( $200 \text{ cells mL}^{-1}$ ) and freshly purified human WBCs ( $5 \times 10^6 \text{ WBCs mL}^{-1}$ ) in a RPMI medium was prepared. For the convenience of cell counting, the H1975 cells were pre-stained with DiO green fluorescent dye. For the convenience of cell counting, the H1975 cells were pre-stained with DiO green fluorescent dye.

The second-type artificial CTC samples were prepared by spiking EpCAM-positive H1975 NSCLC cells (approximately  $200 \text{ cells mL}^{-1}$ ) into freshly collected human blood. Using these artificial samples (H1975 cells in  $1.0 \text{ mL}$  WBCs), we conducted CTC purification/viability studies according to an optimal CTC purification protocol.

**Immunofluorescence Staining of Captured CTCs.** CTCs captured with the Thermoresponsive NanoVelcro system were fixed with PBS containing 2.0% formaldehyde, washed, and blocked with 1% donkey sera in PBS. Then, cells were identified with a commonly used three-color immunofluorescence method including FITC-conjugated anticytokeratin (CK), a marker for epithelial cells, TRITC-conjugated anti-CD45 (CD45, a marker for white blood cells), and DAPI nuclear staining. Combined information was utilized to discriminate tumor cells from WBCs. Cells that were CK+/CD45-/DAPI+ and morphologically intact were identified as CTCs, while cells that exhibited high CD45 and low CK expression levels were WBCs.

**Patient Blood Samples.** For seven patients with histologically confirmed non-small cell lung cancer and genetically confirmed EGFR mutations on tumor specimens, peripheral blood was obtained during therapeutic treatment with written informed consent of the patients. Five milliliters of patient peripheral blood was collected for each time in BD Vacutainer (glass blood collection tubes with acid citrate dextrose, BD Medical, Fisher CAT# 02-684-26) without any treatment. Afterward, the blood sample ( $1.0 \text{ mL}$  for each experiment) was subjected to the purification procedure through the Thermoresponsive NanoVelcro system.

**DNA Extraction, Amplification, and Point Mutation PCR.** Genomic DNAs were first extracted from purified CTC in a patient's peripheral blood after two-round purification in the Thermoresponsive NanoVelcro system and then amplified according to the standard procedure recommended by whole genome amplification kit (REPLI-g, Qiagen). To sequence EGFR exon 20 (covering codon 790) and 21 (covering codon 858) for mutational analysis, the resulting WGA DNA were used to amplify by PCR with two pairs of primers (see Supporting Information). The PCR was carried out in PCR buffer containing 100 ng of WGA DNA, 25 nM primers, and 2x My Taq HS mix (Bioline) using 30 cycles of  $95 \text{ }^\circ\text{C}$  for 30 s,  $55 \text{ }^\circ\text{C}$  for 30 s, and  $72 \text{ }^\circ\text{C}$  for 30 s.

**Conflict of Interest:** The authors declare the following competing financial interest(s): Following the guideline of UCLA Conflict of Interest Review Committee (CIRC), the authors would like to disclose: (i) The intellectual property that arose from this study has been licensed to CytoLumina Technologies Corp.; and (ii) Tom Lee and Hsian-Rong Tseng have their financial interests in CytoLumina Technologies Corp. given their roles as the company founders.

**Acknowledgment.** This work was supported by National Institutes of Health (R21-CA151159, R33-CA157396, P50-CA92131, R33-CA174562, and PO1-CA168585). The research endeavors at RIKEN and Academia Sinica were supported by RIKEN, Academia Sinica, and the Academia Sinica Research Project on Nanoscience and Technology. The research endeavors at Sun Yat-Sen University were supported by National Natural Science Foundation of China (Grants 30900650/H1615 and 81372501/H1615).

**Supporting Information Available:** Information on the custom-designed chip holder, digital fluidic handler, preparation and SEM image of Thermoresponsive NanoVelcro substrates, measurement of contact angles, optimization of Thermoresponsive NanoVelcro CTC purification system, viability and

purity study on purified CTCs, performed mutational analysis (on EGFR gene) using the second-type artificial blood samples, enumeration and molecular analysis of CTCs in NSCLC patients' blood samples, CTC enumeration studies, and CTC-based molecular analysis. This material is available free of charge via the Internet at <http://pubs.acs.org>.

## REFERENCES AND NOTES

- Pantel, K.; Alix-Panabieres, C. Circulating Tumour Cells in Cancer Patients: Challenges and Perspectives. *Trends Mol. Med.* **2010**, *16*, 398–406.
- Speicher, M. R.; Pantel, K. Tumor Signatures in the Blood. *Nat. Biotechnol.* **2014**, *32*, 441–443.
- Cristofanilli, M.; Budd, G. T.; Ellis, M. J.; Stopeck, A.; Matera, J.; Miller, M. C.; Reuben, J. M.; Doyle, G. V.; Allard, W. J.; Terstappen, L. W.; et al. Circulating Tumor Cells, Disease Progression, and Survival in Metastatic Breast Cancer. *N. Engl. J. Med.* **2004**, *351*, 781–791.
- Riethdorf, S.; Fritsche, H.; Muller, V.; Rau, T.; Schindlbeck, C.; Rack, B.; Janni, W.; Coith, C.; Beck, K.; Janicke, F.; et al. Detection of Circulating Tumor Cells in Peripheral Blood of Patients with Metastatic Breast Cancer: A Validation Study of the Cellsearch System. *Clin. Cancer Res.* **2007**, *13*, 920–928.
- Shaffer, D. R.; Leversha, M. A.; Danila, D. C.; Lin, O.; Gonzalez-Espinoza, R.; Gu, B.; Anand, A.; Smith, K.; Maslak, P.; Doyle, G. V.; et al. Circulating Tumor Cell Analysis in Patients with Progressive Castration-Resistant Prostate Cancer. *Clin. Cancer Res.* **2007**, *13*, 2023–2029.
- Maheswaran, S.; Sequist, L. V.; Nagrath, S.; Ulkus, L.; Brannigan, B.; Collura, C. V.; Inserra, E.; Diederichs, S.; Iafraite, A. J.; Bell, D. W.; et al. Detection of Mutations in EGFR in Circulating Lung-Cancer Cells. *N. Engl. J. Med.* **2008**, *359*, 366–377.
- Ni, X.; Zhuo, M.; Su, Z.; Duan, J.; Gao, Y.; Wang, Z.; Zong, C.; Bai, H.; Chapman, A. R.; Zhao, J.; et al. Reproducible Copy Number Variation Patterns among Single Circulating Tumor Cells of Lung Cancer Patients. *Proc. Natl. Acad. Sci. U.S.A.* **2013**, *110*, 21083–21088.
- Bidard, F. C.; Weigelt, B.; Reis-Filho, J. S. Going with the Flow: From Circulating Tumor Cells to DNA. *Sci. Transl. Med.* **2013**, *5*, 207ps214.
- Lohr, J. G.; Adalsteinsson, V. A.; Cibulskis, K.; Choudhury, A. D.; Rosenberg, M.; Cruz-Gordillo, P.; Francis, J. M.; Zhang, C. Z.; Shalek, A. K.; Satija, R.; et al. Whole-Exome Sequencing of Circulating Tumor Cells Provides a Window into Metastatic Prostate Cancer. *Nat. Biotechnol.* **2014**, *32*, 479–484.
- Zhang, L.; Ridgway, L. D.; Wetzel, M. D.; Ngo, J.; Yin, W.; Kumar, D.; Goodman, J. C.; Groves, M. D.; Marchetti, D. The Identification and Characterization of Breast Cancer CTCs Competent for Brain Metastasis. *Sci. Transl. Med.* **2013**, *5*, 180ra148.
- Yu, M.; Bardia, A.; Aceto, N.; Bersani, F.; Madden, M. W.; Donaldson, M. C.; Desai, R.; Zhu, H.; Comaills, V.; Zheng, Z.; et al. Cancer Therapy. *Ex Vivo* Culture of Circulating Breast Tumor Cells for Individualized Testing of Drug Susceptibility. *Science* **2014**, *345*, 216–220.
- Wang, S.; Wang, H.; Jiao, J.; Chen, K. J.; Owens, G. E.; Kamei, K.; Sun, J.; Sherman, D. J.; Behrenbruch, C. P.; Wu, H.; et al. Three-Dimensional Nanostructured Substrates toward Efficient Capture of Circulating Tumor Cells. *Angew. Chem., Int. Ed.* **2009**, *48*, 8970–8973.
- Zhang, N.; Deng, Y.; Tai, Q.; Cheng, B.; Zhao, L.; Shen, Q.; He, R.; Hong, L.; Liu, W.; Guo, S.; et al. Electrospun TiO<sub>2</sub> Nanofiber-Based Cell Capture Assay for Detecting Circulating Tumor Cells from Colorectal and Gastric Cancer Patients. *Adv. Mater.* **2012**, *24*, 2756–2760.
- Sekine, J.; Luo, S. C.; Wang, S.; Zhu, B.; Tseng, H. R.; Yu, H. H. Functionalized Conducting Polymer Nanodots for Enhanced Cell Capturing: The Synergistic Effect of Capture Agents and Nanostructures. *Adv. Mater.* **2011**, *23*, 4788–4792.
- Hsiao, Y.-S.; Luo, S.-C.; Hou, S.; Zhu, B.; Sekine, J.; Kuo, C.-W.; Chueh, D.-Y.; Yu, H.-h.; Tseng, H.-R.; Chen, P. 3D Bioelectronic Interface: Capturing Circulating Tumor Cells onto Conducting Polymer-Based Micro/Nanorod Arrays with Chemical and Topographical Control. *Small* **2014**, *10*, 3012–3017.
- Lin, M.; Chen, J. F.; Lu, Y. T.; Zhang, Y.; Song, J.; Hou, S.; Ke, Z.; Tseng, H. R. Nanostructure Embedded Microchips for Detection, Isolation, and Characterization of Circulating Tumor Cells. *Acc. Chem. Res.* **2014**, *10*, 2941–2950.
- Lee, H.; Jang, Y.; Seo, J.; Nam, J.-M.; Char, K. Nanoparticle-Functionalized Polymer Platform for Controlling Metastatic Cancer Cell Adhesion, Shape, and Motility. *ACS Nano* **2011**, *5*, 5444–5456.
- Park, G.-S.; Kwon, H.; Kwak, D. W.; Park, S. Y.; Kim, M.; Lee, J.-H.; Han, H.; Heo, S.; Li, X. S.; Lee, J. H.; et al. Full Surface Embedding of Gold Clusters on Silicon Nanowires for Efficient Capture and Photothermal Therapy of Circulating Tumor Cells. *Nano Lett.* **2012**, *12*, 1638–1642.
- Banerjee, S. S.; Paul, D.; Bhansali, S. G.; Aher, N. D.; Jalota-Badhwari, A.; Khandare, J. Enhancing Surface Interactions with Colon Cancer Cells on a Transferrin-Conjugated 3D Nanostructured Substrate. *Small* **2012**, *8*, 1657–1663.
- Liu, X.; Chen, L.; Liu, H.; Yang, G.; Zhang, P.; Han, D.; Wang, S.; Jiang, L. Bio-Inspired Soft Polystyrene Nanotube Substrate for Rapid and Highly Efficient Breast Cancer-Cell Capture. *NPG Asia Mater.* **2013**, *5*, e63.
- He, R.; Zhao, L.; Liu, Y.; Zhang, N.; Cheng, B.; He, Z.; Cai, B.; Li, S.; Liu, W.; Guo, S.; et al. Biocompatible TiO<sub>2</sub> Nanoparticle-Based Cell Immunoassay for Circulating Tumor Cells Capture and Identification from Cancer Patients. *Biomed. Microdevices* **2013**, *15*, 617–626.
- Zhang, P.; Chen, L.; Xu, T.; Liu, H.; Liu, X.; Meng, J.; Yang, G.; Jiang, L.; Wang, S. Programmable Fractal Nanostructured Interfaces for Specific Recognition and Electrochemical Release of Cancer Cells. *Adv. Mater.* **2013**, *25*, 3566–3570.
- Yoon, H. J.; Kim, T. H.; Zhang, Z.; Azizi, E.; Pham, T. M.; Paoletti, C.; Lin, J.; Ramnath, N.; Wicha, M. S.; Hayes, D. F.; et al. Sensitive Capture of Circulating Tumor Cells by Functionalized Graphene Oxide Nanosheets. *Nat. Nanotechnol.* **2013**, *8*, 735–741.
- Wang, S.; Liu, K.; Liu, J.; Yu, Z. T.; Xu, X.; Zhao, L.; Lee, T.; Lee, E. K.; Reiss, J.; Lee, Y. K.; et al. Highly Efficient Capture of Circulating Tumor Cells by Using Nanostructured Silicon Substrates with Integrated Chaotic Micromixers. *Angew. Chem., Int. Ed.* **2011**, *50*, 3084–3088.
- Lu, Y. T.; Zhao, L.; Shen, Q.; Garcia, M. A.; Wu, D.; Hou, S.; Song, M.; Xu, X.; Ouyang, W. H.; Ouyang, W. W.; et al. Nanovelcro Chip for Ctc Enumeration in Prostate Cancer Patients. *Methods* **2013**, *64*, 144–152.
- Stroock, A. D.; Dertinger, S. K.; Ajdari, A.; Mezic, I.; Stone, H. A.; Whitesides, G. M. Chaotic Mixer for Microchannels. *Science* **2002**, *295*, 647–651.
- Hou, S.; Zhao, L.; Shen, Q.; Yu, J.; Ng, C.; Kong, X.; Wu, D.; Song, M.; Shi, X.; Xu, X.; et al. Polymer Nanofiber-Embedded Microchips for Detection, Isolation, and Molecular Analysis of Single Circulating Melanoma Cells. *Angew. Chem., Int. Ed.* **2013**, *52*, 3379–3383.
- Zhao, L.; Lu, Y. T.; Li, F.; Wu, K.; Hou, S.; Yu, J.; Shen, Q.; Wu, D.; Song, M.; Ouyang, W. H.; et al. High-Purity Prostate Circulating Tumor Cell Isolation by a Polymer Nanofiber-Embedded Microchip for Whole Exome Sequencing. *Adv. Mater.* **2013**, *25*, 2897–2902.
- Hou, S.; Zhao, H.; Zhao, L.; Shen, Q.; Wei, K. S.; Suh, D. Y.; Nakao, A.; Garcia, M. A.; Song, M.; Lee, T.; et al. Capture and Stimulated Release of Circulating Tumor Cells on Polymer-Grafted Silicon Nanostructures. *Adv. Mater.* **2013**, *25*, 1547–1551.
- Okano, T.; Yamada, N.; Okuhara, M.; Sakai, H.; Sakurai, Y. Mechanism of Cell Detachment from Temperature-Modulated, Hydrophilic-Hydrophobic Polymer Surfaces. *Biomaterials* **1995**, *16*, 297–303.
- Sheng, W.; Ogunwobi, O. O.; Chen, T.; Zhang, J.; George, T. J.; Liu, C.; Fan, Z. H. Capture, Release and Culture of Circulating Tumor Cells from Pancreatic Cancer Patients Using an Enhanced Mixing Chip. *Lab Chip* **2014**, *14*, 89–98.



32. Kamangar, F.; Dores, G. M.; Anderson, W. F. Patterns of Cancer Incidence, Mortality, and Prevalence across Five Continents: Defining Priorities To Reduce Cancer Disparities in Different Geographic Regions of the World. *J. Clin. Oncol.* **2006**, *24*, 2137–2150.
33. Jemal, A.; Siegel, R.; Ward, E.; Hao, Y.; Xu, J.; Thun, M. J. Cancer Statistics, 2009. *CA Cancer J. Clin.* **2009**, *59*, 225–249.
34. Pao, W.; Chmielecki, J. Rational, Biologically Based Treatment of EGFR-Mutant Non-Small-Cell Lung Cancer. *Nat. Rev. Cancer* **2010**, *10*, 760–774.
35. Hirsch, F. R.; Bunn, P. A., Jr. EGFR Testing in Lung Cancer Is Ready for Prime Time. *Lancet Oncol.* **2009**, *10*, 432–433.
36. Cross, D. A.; Ashton, S. E.; Ghiorghiu, S.; Eberlein, C.; Nebhan, C. A.; Spitzler, P. J.; Orme, J. P.; Finlay, M. R.; Ward, R. A.; Mellor, M. J.; *et al.* Azd9291, an Irreversible EGFR TKI, Overcomes T790m-Mediated Resistance to EGFR Inhibitors in Lung Cancer. *Cancer Discovery* **2014**, *4*, 1046–1061.
37. Walter, A. O.; Sjin, R. T.; Haringsma, H. J.; Ohashi, K.; Sun, J.; Lee, K.; Dubrovskiy, A.; Labenski, M.; Zhu, Z.; Wang, Z.; *et al.* Discovery of a Mutant-Selective Covalent Inhibitor of EGFR That Overcomes T790m-Mediated Resistance in NSCLC. *Cancer Discovery* **2013**, *3*, 1404–1415.
38. Wang, S.; Liu, K.; Liu, J.; Yu, Z. T.-F.; Xu, X.; Zhao, L.; Lee, T.; Lee, E. K.; Reiss, J.; Lee, Y.-K.; *et al.* Highly Efficient Capture of Circulating Tumor Cells by Using Nanostructured Silicon Substrates with Integrated Chaotic Micromixers. *Angew. Chem., Int. Ed.* **2011**, *50*, 3084–3088.
39. Xia, Y.; Whitesides, G. M. Soft Lithography. *Annu. Rev. Mater. Sci.* **1998**, *28*, 153–184.
40. Peng, K.-Q.; Yan, Y.-J.; Gao, S.-P.; Zhu, J. Synthesis of Large-Area Silicon Nanowire Arrays via Self-Assembling Nanoelectrochemistry. *Adv. Mater.* **2002**, *14*, 1164–1167.